to[2b] $f^{-1}\int_{R_{core}}^{R_{core}+L}\zeta^{-3}r^2\,dr \approx f^{1/2}\ln(R_{core}+L)/R_{core}$ where L is the thickness of the corona. Strictly speaking, the Daoud–Cotton model is applicable only to micelles endowed with thick coronas, $L \gg R_{core}$. Nevertheless, this approach recovers the Alexander–de Gennes results in the limit of $L \ll R_{core}$ when the corona is essentially a flat grafted layer. This, however, is not crucial to our discussion as F_{corona} is negligible in this limit.

The micelle's equilibrium structure is determined by minimizing F with respect to f. To simplify the algebra, we approximate the logarithmic factor in (1) as a constant. This yields the scaling behavior of the equilibrium f and thus of R_{core} and L. Two extreme micellar types are distinguishable: (i) micelles with thin coronas, $L \ll R_{core}$, for which F_{core} is the dominant penalty term; and (ii) starlike micelles endowed with extended coronas, $L \gg R_{core}$, where the major penalty term is F_{corona}. The scaling behavior of f is different in the two limits:[2]

$$f \sim N_B \qquad L \ll R_{core} \tag{2i}$$

$$f \sim N_B^{4/5} \qquad L \gg R_{core} \tag{2ii}$$

So far we have considered the equilibrium structure of micelles in a pure low molecular weight solvent. Addition of A homopolymers to the solution does not affect F_{core} and $F_{interface}$ but does modify F_{corona}. In turn, the effect on F_{corona} is important only for starlike micelles. For brevity we will thus consider the effect of immersion in a solution of A homopolymers consisting each of N_A monomers on starlike micelles. Such solutions, of concentration $c > c^*$, may be considered as a melt of "concentration blobs". Each blob consists of $n_b \approx (ca^3)^{-3/4}$ monomers and is of size $\xi_c \approx (ca^3)^{-3/4}a$. The presence of homopolymers in the solution results in increased screening of excluded volume interactions in the corona. Within the Daoud–Cotton model this effect is accounted for by distinguishing two coronal regions:[5] an interior region where the star structure is preserved (i.e., $\xi \approx r/f^{1/2}$) and an exterior region where the coronal blocks assume bulk structure (i.e., $\xi \approx \xi_c$). The crossover between the two zones occurs when the size of the coronal blobs equals that of the concentration blobs, $\xi \approx \xi_c$. This takes place at a distance $\chi \approx (ca^3)^{-3/4}f^{1/2}a$ from the micelle's center. In this case F_{corona}, as obtained by the blob counting ansatz, is given by

$$F_{corona}/kT \approx f^{1/2}\ln \chi/R_{core} + (N - N_i)/n_b - N/n_b \tag{3}$$

where N_i is the number of monomers per block in the inner, starlike region (i.e., $r < \chi$). The extent of the starlike region, χ, and the magnitude of F_{corona} diminish with the growing homopolymer concentration c. This process is associated with an increase of the aggregation number f. However, the growth in f is eventually arrested by the second penalty term, F_{core}. Altogether, the aggregation number of starlike micelles grows from $f \sim N_B^{4/5}$ in a pure low molecular weight solvent to $f \sim N_B$ in an A homopolymer solution of concentration $c \sim N_B^{-2/9}a^{-3}$. At this stage f and R_{core} of the starlike micelles scale exactly as those of micelles with thin coronas. The overall dimensions of the two micellar types remain, however, different because the coronal contribution to the diameter of starlike micelles is always significant.[5] The effect considered is only observable if the micelles attain their equilibrium structure. To ensure that, care should be taken to operate above the glass temperature of the core blocks. Also, N_B should not be too large as the relevant relaxation times scale as[7] $\exp(\gamma a^2 N_B^{2/3}/kT)$.

References and Notes

(1) Tanford, C. *The Hydrophobic Effect*, 2nd ed.; Wiley: New York, 1980.
(2) (a) Halperin, A. *Macromolecules* **1987**, *20*, 2943. (b) Marques, C.; Joanny, J. F.; Leibler, L. *Macromolecules* **1988**, *21*, 1051.
(3) de Gennes, P.-G. In *Solid State Physics*; Liebert, L., Ed.; Academic: New York, 1978; Supplement 14.
(4) Semenov, A. N. *Sov. Phys.—JETP (Engl. Transl.)* **1985**, *61*, 733.
(5) Daoud, M.; Cotton, J. P. *J. Phys. (Les Ulis, Fr.)* **1982**, *43*, 531.
(6) Witten, T. A.; Pincus, P. A. *Macromolecules* **1986**, *19*, 2509.
(7) Halperin, A.; Alexander, S. *Macromolecules*, in press.

NMR Characterization of Molecular Motions in Liquid-Crystalline Poly(ester amides) below Their Glass Transition

GALEN R. HATFIELD*,† and SHAUL M. AHARONI

Corporate Technology, Allied-Signal Inc., Morristown, New Jersey 07960.

Received December 14, 1988; Revised Manuscript Received February 23, 1989

Introduction

A new family of poly(ester amides) has been recently synthesized and shown to exhibit thermotropic liquid crystallinity.[1] These poly(ester amides) are highly regular, strictly alternating, and interchain hydrogen bonded, with the generic structure given below:

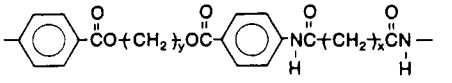

When $y = 2$, the transition from semicrystalline solid to isotropic melt occurs in a single step. However, for $y \geq 3$ this transformation occurs in several steps, during some of which the polymers were found to exhibit thermotropic liquid crystallinity.[1,2] These steps are first-order phase transitions, the number and magnitude of which depend on the lengths of x and y.[2]

Many of the structural details of this system have been elucidated through a combination of solid-state nuclear magnetic resonance (NMR), infrared (IR), and X-ray diffraction (XRD) studies.[1-3] IR results reveal that the amide groups are hydrogen bonded in the crystalline, glassy, and mesomorphic states while XRD results suggest that the hydrogen bonds exist between chains and are not present as intrachain bonds. By a combination of NMR and XRD, it was determined that the conformation of the x methylenes is exclusively trans but that the y segments include both trans and gauche states. The gauche bonds allow the chains to adopt an overall zigzag configuration and are associated with the existence of liquid crystallinity.[3]

Previously inaccessible information such as amorphous-phase structure and polymer-chain dynamics can often be readily obtained through a variety of NMR methods.[4,5] One of the strengths of solid-state NMR is its ability to probe molecular motion at specific individual nuclear sites along a polymer chain. This is often done by measuring $T_{1\rho}$(C), or ^{13}C spin–lattice relaxation in the rotating frame.[6,7] Studies of $T_{1\rho}$(C) have provided valuable information on molecular dynamics in semicrystalline polymers such as polyesters and in glassy polymers such as polycarbonates and polystyrenes. The purpose of this report is to document our findings on motional behavior in poly(ester amides) in their semicrystalline solid state below their glass transition temperature, T_g. In addition,

† Current address: Washington Research Center, W. R. Grace & Co., 7379 Route 32, Columbia, MD 21044.

0024-9297/89/2222-3807$01.50/0

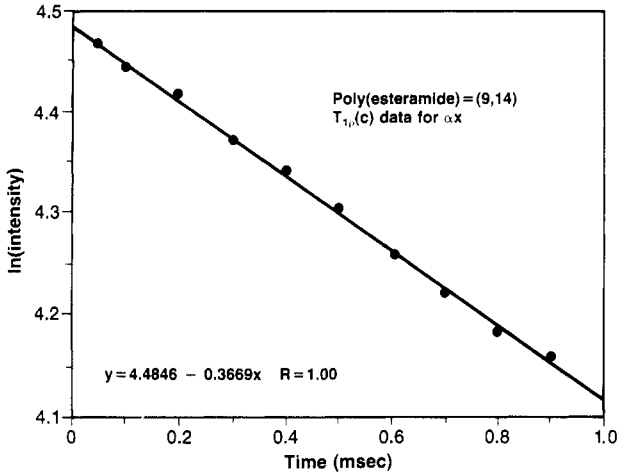

Figure 1. Representative $\langle T_{1\rho}(C)\rangle$ data.

some intriguing observations regarding segmental motion in these liquid-crystalline polymers is also presented.

Experimental Section

NMR Spectroscopy. Solid-state ^{13}C NMR spectra were obtained using cross-polarization (CP) and magic angle spinning (MAS) techniques[8-10] at 50.3 MHz on a Varian XL200 spectrometer equipped with Doty Scientific solids accessories. The magic angle was adjusted to within 0.1° using the ^{79}Br spectrum of KBr.[11] CP/MAS spectra were acquired at room temperature using spinning speeds of 3.5–4.5 kHz, a 2-ms contact time, and a 2-s repetition time.

Measurements of ^{13}C spin–lattice relaxation in the rotating frame were performed according to literature methods.[6,7] These experiments were performed at 30 °C with a proton radio frequency (rf) field of 41.6 kHz. Spinning speeds of 4.00 ± 0.01 kHz were used on all samples to standardize the effect of MAS on $T_{1\rho}(C)$. Values for $\langle T_{1\rho}(C)\rangle$, the average $T_{1\rho}(C)$, were determined from a least-squares analysis of a plot of ln intensity vs τ, the time during which the carbon rf field is maintained after CP. A representative plot is given in Figure 1. The times τ ranged from 0.05 to 0.9 ms. Note that the fit to a straight line is very good. Spectra of high signal to noise ratios were acquired for all samples in order to ensure the accuracy of the $\langle T_{1\rho}(C)\rangle$ measurement. The values of $\langle T_{1\rho}(C)\rangle$ reported for the aromatic carbons are taken from the average of the two protonated sites. The other aromatic sites bear no directly attached protons. Thus, the relaxation mechanisms for these carbons (as well as the carbonyls) are open to question, and the relationship between $\langle T_{1\rho}(C)\rangle$ and motion becomes more speculative.[12]

Samples. The samples investigated here were powders and were prepared as described elsewhere.[1]

Results and Discussion

Carbon–13 spin–lattice relaxation in the rotating frame is a sensitive marker for molecular motion in the mid-kilohertz range.[6,7] This process is characterized by the rate constant $T_{1\rho}(C)^{-1}$ and is typically reported as the average value, $\langle T_{1\rho}(C)\rangle$.[6,13] It is important to note that $T_{1\rho}(C)$ cannot always be considered to be purely dependent upon molecular motion, since spin–spin processes may also contribute to $T_{1\rho}(C)$.[6,7,14-16] Fortunately, the literature reveals that spin–spin processes usually play a dominant role only in highly crystalline polymers[14,15] or at low temperatures.[16] The room-temperature relaxation of many glassy and semicrystalline polymers,[6,7,12,17-22] on the other hand, has been shown to be dominated by motional processes. These polymers include the semicrystalline aromatic polyesters hytrel,[12,13] poly(butadieneterephthalate)[12,13] and poly(ethyleneterephthalate),[20] which are in many ways analogous to the poly(ester amides) under study here. A detailed treatment of spin–lattice relaxation in the rotating frame is available elsewhere[23] and will not

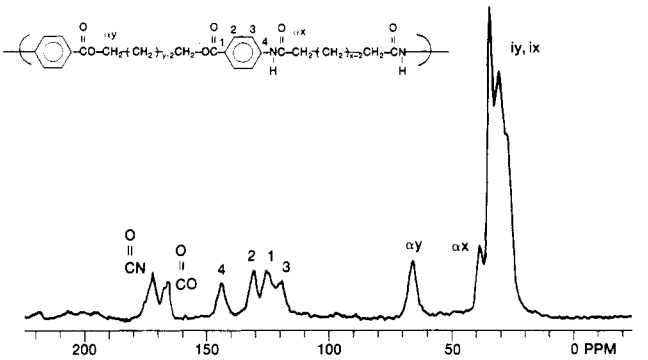

Figure 2. ^{13}C CP/MAS NMR spectrum of the poly(ester amide) (4, 14).

Table I
Poly(ester amide) Chemical Shift Assignments

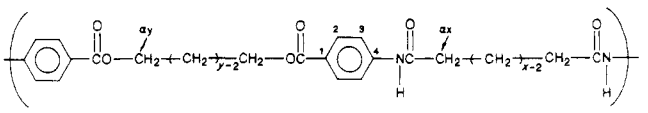

carbon	chemical shift,[a] ppm	carbon	chemical shift,[a] ppm
C(O)O	166	4	143
C(O)N	172	αy	61, 65[b]
1	125	αx	38
2	131	iy,ix	35–23
3	119		

[a] Relative to TMS to 0 ppm. [b] See ref 3.

be repeated here. It is noted, however, that $\langle T_{1\rho}(C)\rangle$ is directly related to the correlation coefficient and thereby inversely proportional to molecular motion. It is also important to note that $\langle T_{1\rho}(C)\rangle$ reflects an average of the motional heterogeneity that exists for each individual carbon type and thereby an average for the entire polymeric system.

The motional behavior of 11 poly(ester amides) has been investigated in this study. These systems are characterized by the length of the methylene x and y segments and will hereafter be referred to as (y,x). The ^{13}C CP/MAS NMR spectra of these polymers are similar, and the spectrum of (4, 14) is given as an example in Figure 2. Assignments based on model compounds[3] and dipolar dephasing experiments[24] (not shown) are given in Table I. In this work, we are concerned with the motional behavior of three key moieties in the poly(ester amide) system: the aromatic ring, the ester chain, and the amide chain. The resonances due to the aromatic carbons are well resolved, as are the methylenes adjacent to the ester (αy) and amide (αx) functionalities. However, when x or y exceeds 2, peaks from the interior (ix, iy) methylenes overlap. Thus, in order to avoid any complications, only the αx and αy carbons will be considered. The peaks corresponding to each of these carbons are indicated in Figure 2.

Values of $\langle T_{1\rho}(C)\rangle$ were determined for each of these moieties in 11 poly(ester amides). As mentioned above, the physical properties of these polymers are strongly dependent upon the length of x and y. We first begin by considering two families: one of short x ($x = 4$) and one of long x ($x = 14$). Plots of $\langle T_{1\rho}(C)\rangle$ for a series of y within each of these families are given in Figures 3 and 4. Several interesting trends can be observed that provide insight into molecular motion in poly(ester amides).

For all combinations of (y,x), mobility at the αy (ester) site appears to be more restricted than at the αx (amide) site. It was previously determined[3] that in the crystalline and mesomorphic states the amide methylenes (x) are

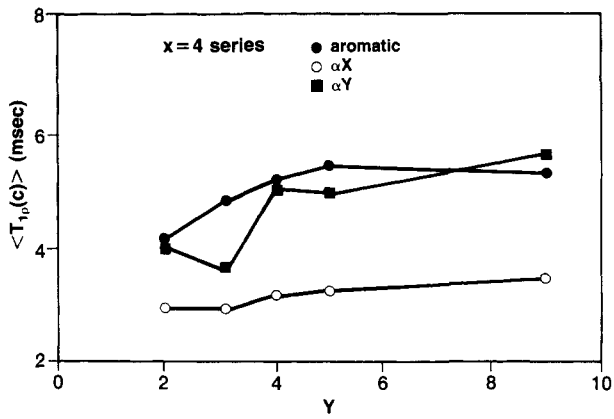

Figure 3. Plots of $\langle T_{1\rho}(C)\rangle$ for the three key moieties of poly(ester amides) when x is short (4) and y is varied.

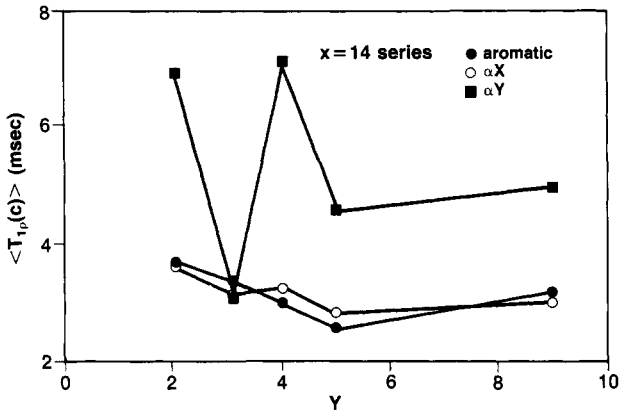

Figure 4. Plots of $\langle T_{1\rho}(C)\rangle$ for the three key moieties of poly(ester amides) when x is long (14) and y is varied.

exclusively trans while the ester methylenes (y) contain both trans and gauche states. The full extension of the amide chain may simply provide more freedom for movement than is possible in the kinked or twisted ester portion. It is interesting to note, however, that motion at the αx (amide) site changes little from short x (Figure 3) to long x (Figure 4). This suggests that the effects governing mobility at the αx site are relatively short ranged in nature. This is also evidenced by the fact that the values of $\langle T_{1\rho}(C)\rangle$ at αx are largely independent of the length of the ester (y) chain.

While mobility at the amide site appears to be essentially constant, the dynamics of the aromatic ring were found to be dependent upon (y,x). In both the long and short x series, $\langle T_{1\rho}(C)\rangle$ for the aromatic ring showed a slightly greater variation with y than those obtained for the αx site. The most significant change, however, is best seen by comparing Figures 3 and 4. Note that for all y, when x is changed from short (x = 4) to long (x = 14), there is a substantial increase in motion at the aromatic ring. There are two plausible explanations to account for this behavior. The first is that motion at the aromatic site is governed by the amide chain and only marginally influenced by the ester chain. This may again be due to the fact that the amide region is extended, providing more degrees of freedom. Such an explanation would require that the forces governing motion at the aromatic site are long ranged in nature and directly related to the amide chain. A second explanation is that, as x increases, the interchain interactions decrease, providing a mode for increased aromatic motion. Thermal studies[1,2] reveal that an increase in x results in a corresponding increase in the number and decrease of the magnitude of thermal transitions. This may be indicative of a weakening of interchain interactions.

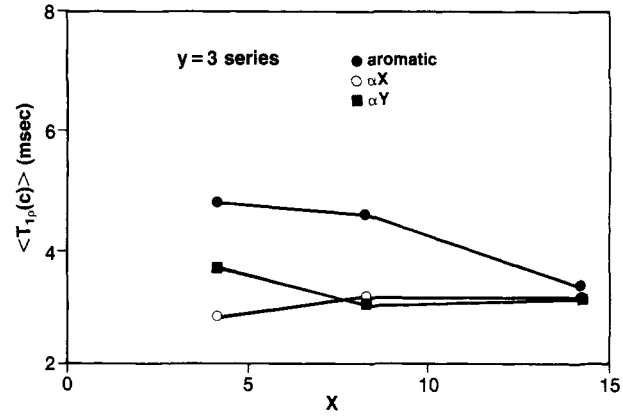

Figure 5. Plots of $\langle T_{1\rho}(C)\rangle$ for the three key moieties of poly(ester amides) when y is short (3) and x is varied.

The most intriguing trend in Figures 3 and 4 is clearly the behavior of the ester αy site. When x is short (Figure 3), there is a slight oscillation in $\langle T_{1\rho}(C)\rangle$. When x is long (Figure 4), the same type of oscillation is present but dramatically amplified. These changes correspond to an "odd–even effect" in which motion becomes more restricted for even values of y. This odd–even behavior was also observed (not shown) in related experiments (i.e., other temperatures, different B_1 values). The fact that the oscillation is more pronounced for long x may be related to the increased molecular mobility observed for the aromatic ring. As motion at the ring increases and interchain interactions decrease, the factors governing the odd–even effect become more prevalent and the changes in molecular dynamics become more pronounced. The nature, potential causes, and significance of this motional odd–even behavior will be discussed below.

A third family in which x is varied instead of y was also investigated in this study. Shown in Figure 5 are the plots of $\langle T_{1\rho}(C)\rangle$ for a series of x when y is short (y = 3). Unfortunately, there are less data points available in this study. However, one can see that as x is increased there is a "homogenizing" of segmental motion. When the amide chain is short, varying degrees of segmental motion are present, which "wash away" when the chain becomes long. Again, this may reflect a weakening of interchain interactions that appears to accompany an increase in x.

Odd–Even Effect. The data presented in Figures 3 and 4 reveal that an intriguing motional odd–even behavior exists at the ester (αy) site that is absent from the amide (αx) and aromatic moieties. We have previously shown[1,2] that the thermal behavior of poly(ester amides) is strongly dependent upon the length of y and x. Examination of that data reveals that the poly(ester amides) with y = 2, 4, and 9 behave differently from those with y = 3 and 5. In the cases where y = 2, 4, or 9, the polymers exhibit either one or very few endothermic transitions between room temperature and the isotropic melt. However, when y = 3 or 5, the polymers exhibit many endotherms. In addition, the number of such transitions increases as x increases. For example, there are 11 endotherms in the heating cycle of y = 5, x = 14. The differences between the two sets of y families appear to be reflected in the motional dynamics of the ester (αy) site, as illustrated in Figures 3 and 4. The αy site in the polymers with y = 2 and 4 are clearly more rigid (in progression) than those with y = 3 and 5. Further, this difference is more pronounced when x is long (Figure 4), which may be responsible for the higher number of endotherms observed for

cases of $y = 3$ or 5 and $x = 14$.

Liquid crystallinity is observed in those poly(ester amides) exhibiting at least two endotherms during heating. The larger the number of such transitions, the clearer the mesomorphic behavior. This is seen as birefringence in cross-polarized light coexisting with polymer mobility. Of the polymers given in Figures 3 and 4, optically observable liquid crystallinity in the form of birefringence coupled with spontaneous fluidity is evident in the cases where $y = 3$ and $y = 5$. Birefringence is also observed but associated with slow mobility when $y = 9$. No such optically observable mesomorphic behavior is observed in the studied polymers when $y = 2$ and $y = 4$. Thus, we are led to the conclusion that when mobility at the ester (αy) site is restricted, as is the case for $y = 2$ and $y = 4$, the polymers melt in a single step at relatively high temperatures. However, when the αy carbon is more mobile, as is the case in $y = 3$, $y = 5$, and probably $y = 9$, then libration occurs in several small increments covering a broad temperature interval.

These results indicate a relationship between mesomorphic behavior in poly(ester amides) and molecular dynamics in the ester moiety. This suggests that liquid crystallinity is coupled to the molecular dynamics of the ester portion and effectively decoupled from the segmental motion present in the amide and aromatic portions of the polymer chain.

Comparison with Related Systems. It is of interest to compare these results with those previously reported in related studies[12,25–27] of polyesters. Horii and co-workers[25] examined a series of terephthalic acid polyesters above T_g via traditional high-resolution NMR methods. When the nomenclature adopted here is used, these polymers have the general structure $[COC_6H_4COO(CH_2)_yO]$ and are analogous to the aromatic and y fragments of poly(ester amides). They found that, in the mobile isotropic phase above T_g, motion at the aromatic, αy, and iy sites was dependent upon the choice of y. This is the case for poly(ester amides), even below T_g. Further, motion at the aromatic site was greater than at αy. This is the same as our finding when x is long (Figure 4). There are two interesting points here. The first is that different degrees of localized motion, analogous to those observed here for poly(ester amides), also exist in polyesters. The second involves the fact that the motional heterogeneities observed by Horii and co-workers[25] above T_g were also observed by Jelinski and co-workers[12,26,27] on these and related glassy polymers below T_g, suggesting that the motional behavior that predominates below T_g persists above T_g. Unfortunately, our work on poly(ester amides) was limited to the semicrystalline solid state below T_g. However, it is interesting to speculate that these motions may also persist into the thermotropic liquid-crystalline phase. This speculation clearly mandates the need for further study.

Conclusions

It has been demonstrated that the molecular dynamics of poly(ester amides) are internally heterogeneous and dependent upon the length of the amide (x) and ester (y) alkylene chains. Mobility at the amide site was shown to be high relative to the rest of the molecule and largely independent of (y,x). Motion at the aromatic and ester sites, on the other hand, depends upon (y,x). This dependence includes an intriguing odd–even behavior for the ester moiety, revealing that motion at the ester site is more restricted for even values of y. These observations are discussed in terms of a dynamic model for poly(ester amides) and their relationship to related systems.

Registry No. Poly(ester amide) ($y = 2$, $x = 4$), 114677-81-5; poly(ester amide) ($y = 3$, $x = 4$), 114677-89-3; poly(ester amide) ($y = 4$, $x = 4$), 114678-01-2; poly(ester amide) ($y = 5$, $x = 4$), 114678-10-3; poly(ester amide) ($y = 9$, $x = 4$), 114678-21-6; poly(ester amide) ($y = 2$, $x = 14$), 114677-84-8; poly(ester amide) ($y = 3$, $x = 14$), 114677-97-3; poly(ester amide) ($y = 4$, $x = 14$), 114678-08-9; poly(ester amide) ($y = 5$, $x = 14$), 114678-18-1; poly(ester amide) ($y = 9$, $x = 14$), 114678-25-0; poly(ester amide) ($y = 3$, $x = 8$), 114677-93-9.

References and Notes

(1) Aharoni, S. M. *Macromolecules* **1988**, *21*, 1941.
(2) Aharoni, S. M. *Macromolecules* **1989**, *22*, 1125.
(3) Aharoni, S. M.; Correale, S. T.; Hammond, W. B.; Hatfield, G. R.; Murthy, N. S. *Macromolecules* **1989**, *22*, 1137.
(4) Fyfe, C. A. *Solid-State NMR for Chemists*; CFC Press: Guelph, Canada, 1983.
(5) Komoroski, R. A., Ed. *High Resolution NMR Spectroscopy of Synthetic Polymers in Bulk*; VCH Publishers: Deerfield Beach, FL, 1986.
(6) Schaefer, J.; Stejskal, E. O.; Buchdahl, R. *Macromolecules* **1977**, *10*, 384.
(7) Schaefer, J.; Stejskal, E. O.; Steger, T. R.; Sefcik, M. D.; McKay, R. A. *Macromolecules* **1980**, *13*, 1121.
(8) Pines, A.; Gibby, M. G.; Waugh, J. S. *J. Chem. Phys.* **1973**, *59*, 569.
(9) Schaefer, J.; Stejskal, E. O. *J. Am. Chem. Soc.* **1976**, *98*, 1031.
(10) Schaefer, J.; Stejskal, E. O. *Topics in Carbon-13 NMR Spectroscopy*; Levy, G. C., Ed.; Wiley: New York, 1979; Vol. I.
(11) Frye, J. S.; Maciel, G. E. *J. Magn. Reson.* **1982**, *48*, 125.
(12) Jelinski, L. W.; Dumais, J. J.; Watnick, P. I.; Engel, A. K.; Sefcik, M. D. *Macromolecules* **1983**, *16*, 409.
(13) Bovey, F. A.; Jelinski, L. W. *J. Phys. Chem.* **1985**, *89*, 571.
(14) VanderHart, D. L.; Garroway, A. N. *J. Chem. Phys.* **1979**, *71*, 2773.
(15) Schaefer, J.; Sefcik, M. D.; Stejskal, E. O.; McKay, R. A. *Macromolecules* **1984**, *17*, 1118.
(16) Lyerla, J. R. In *High Resolution NMR Spectroscopy of Synthetic Polymers in Bulk*; Komoroski, R. A., Ed.; VCH Publishers: Deerfield Beach, FL, 1986.
(17) Schaefer, J.; Stejskal, E. O.; McKay, R. A.; Dixon, W. T. *Macromolecules* **1984**, *17*, 1479.
(18) Schaefer, J.; Sefcik, M. D.; Stejskal, E. O.; McKay, R. A.; Dixon, W. T.; Cais, R. E. *Macromolecules* **1984**, *17*, 1107.
(19) Havens, J. R.; Koenig, J. L. *Appl. Spectrosc.* **1983**, *37*, 226.
(20) Sefcik, M. D.; Schaefer, J.; Stejskal, E. O.; McKay, R. A. *Macromolecules* **1980**, *13*, 1132.
(21) Steger, T. R.; Schaefer, J.; Stejskal, E. O.; McKay, R. A. *Macromolecules* **1980**, *13*, 1127.
(22) Schaefer, J.; Stejskal, E. O.; Buchdahl, R. *Macromolecules* **1975**, *8*, 291.
(23) Mehring, M. *Principles of High Resolution NMR in Solids*; Springer: Berlin, 1983.
(24) Opella, S. J.; Frey, M. H. *J. Am. Chem. Soc.* **1979**, *101*, 5854.
(25) Horii, F.; Hirai, A.; Murayama, K.; Kitamaru, R.; Suzuki, T. *Macromolecules* **1983**, *16*, 273.
(26) Jelinski, L. W. *Macromolecules* **1981**, *14*, 1341.
(27) Jelinski, L. W.; Dumais, J. J. *Polym. Prepr. (Am. Chem. Soc., Div. Polym. Chem.)* **1981**, *22*, 273.

Comments on "Temperature-Dependent Changes in the Structure of the Amorphous Domains of Semicrystalline Polymers"

JENS RIEGER

FR 11.1 Theoretische Physik, Universität des Saarlandes, 6600 Saarbrücken, FRG

MARC L. MANSFIELD*

Michigan Molecular Institute, 1910 West St. Andrews Road, Midland, Michigan 48640.

Received April 11, 1989; Revised Manuscript Received April 12, 1989

The premelting phenomenon is a spontaneous growth of the amorphous domains of semicrystalline polymers at the expense of the crystalline layers as the temperature

0024-9297/89/2222-3810$01.50/0